Delta9-tetrahydrocannabinol modulates the proteasome system in the brain

V. Salgado-Mendialdúa[1], J. Aguirre-Plans[2], E. Guney[2], R. Reig-Viader[3,4], R. Maldonado[1], À. Bayés[3,4], B. Oliva[2], A. Ozaita[1*]

[1]Laboratory of Neuropharmacology, Dept. Experimental and Health Sciences, Universitat Pompeu Fabra, Parc de Recerca Biomèdica de Barcelona, 08003 Barcelona, Spain

[2]Structural Bioinformatics Laboratory, Biomedical Informatics Research Unit, Parc de Recerca Biomèdica de Barcelona, 08003 Barcelona, Spain

[3]Molecular Physiology of the Synapse Laboratory, Biomedical Research Institute Sant Pau (IIB Sant Pau), Sant Antoni Maria Claret 167, 08025 Barcelona, Spain.

[4]Universitat Autònoma de Barcelona, Cerdanyola del Vallès, 08193 Bellaterra, Spain.

*Corresponding author: Andrés Ozaita. Laboratory of Neuropharmacology-NeuroPhar. Department of Experimental and Health Sciences. Univ. Pompeu Fabra. C/Dr Aiguader 88, 08003 Barcelona, Spain. Phone: 34-93-316-0823; Fax: 34-93-316-0901; E-mail: andres.ozaita@upf.edu; ORCID: 0000-0002-2239-7403

LINK: http://sbi.upf.edu/data/cannabinoid_effects/

Abstract

Cannabis is the most consumed illicit drug worldwide. Its principal psychoactive component, Δ^9-tetrahydrocannabinol (THC), affects multiple brain functions, including cognitive performance, by modulating cannabinoid type-1 (CB1) receptors. These receptors are strongly enriched in presynaptic terminals, where they modulate neurotransmitter release. We analyzed, through a proteomic screening of hippocampal synaptosomal fractions, those proteins and pathways modulated 3 hours after a single administration of an amnesic dose of THC (10 mg/kg, i.p.). Using an isobaric labeling approach, we identified 2,040 proteins, 1,911 of them previously reported in synaptic proteomes, confirming the synaptic content enrichment of the samples. Initial analysis revealed a significant alteration of 122 proteins, where 42 increased and 80 decreased their expression. Gene set enrichment analysis indicated an over-representation of mitochondrial associated functions and cellular metabolic processes. A second analysis focusing on extreme changes revealed 28 proteins with altered expression after THC treatment, 15 of them up-regulated and 13 down-regulated. Using a network topology-based scoring algorithm we identified those proteins in the mouse proteome with the greatest association to the 28 modulated proteins. This analysis pinpointed a significant alteration of the proteasome function, since top scoring proteins were related to the proteasome system (PS), a protein complex involved in ATP-dependent protein degradation. In this regard, we observed that THC decreases 20S proteasome chymotrypsin-like protease activity in the hippocampus. Our data describe for the first time the modulation of the PS in the hippocampus following THC administration under amnesic conditions that may contribute to an aberrant plasticity at synapses.

Keywords: THC, cannabinoid, synaptic proteome, proteasome, hippocampus, proteostasis

1. Introduction

Cannabis sativa preparations are broadly consumed for recreational purposes worldwide [1,2]. In addition, their use in medicinal forms is currently under close scrutiny [3]. Δ^9-tetrahydrocannabinol (THC) is the main psychoactive compound in cannabis preparations [4,5], acting as a partial agonist of cannabinoid type-1 (CB1) and cannabinoid type-2 (CB2) receptors, the principal receptors of the endocannabinoid system [5,6]. CB1 receptors are the most abundant cannabinoid receptors in the brain [7]. These receptors have been localized at presynaptic terminals [8] where they modulate the release of different neurotransmitters based on the local synaptic activity of endocannabinoids, which are lipid messengers working as endogenous agonists [9,10]. CB1 receptors have also been described in mitochondria where they modulate energy metabolism [11,12]. THC administration, acting through CB1 receptors, affects cognitive performance in preclinical and clinical studies [13,14]. The hippocampus, a key brain area for learning and memory, is a relevant target for this deleterious effect of THC on memory performance, since its intrahippocampal administration reproduces the spatial memory deficits caused by systemic THC administration [15]. This amnesic-like effect of THC is mediated by CB1 receptors as it can be prevented by an intrahippocampal injection of a CB1 receptor antagonist [16].

At the biochemical level, THC administration, at doses that produce amnesic-like effects, enhances the activity of several signaling pathways such as the phosphatidylinositol-3-kinase (PI3K)/Akt pathway and the mammalian target of rapamycin (mTOR) pathway, and increases translation initiation landmarks [17–19]. These signaling pathways have been involved in synaptic plasticity processes [20]. Paradoxically, the activation of TORC1 and protein synthesis, under physiological conditions, is necessary for long-term forms of synaptic plasticity [21–23], contributing

to strengthening synaptic connections necessary for memory storage [24]. At the mitochondrial level, THC reduces the activity of electron transport chain complexes [25]. Moreover, THC also reduces cellular respiration by inhibiting protein kinase A (PKA)-dependent phosphorylation of specific subunits of the mitochondrial electron transport system. Finally, mitochondrial CB1R (mtCB1R) was found to mediate the working memory impairment produced by cannabinoids, linking mitochondrial activity deregulation to the cognitive alterations produced by THC [26]. Thus, THC affects the fine balance between synaptic plasticity and metabolic pathways necessary for memory formation.

In order to study this effect of THC on protein expression, we analyzed the hippocampal synaptosomal proteome shortly after a single administration of an amnesic dose of THC. Analysis of the modulated proteins revealed a preponderant representation of cellular metabolism-associated pathways. Additional analysis pointed to the proteasome system (PS), which activity was affected by THC. These results reveal a relevant short-term effect of THC on hippocampal metabolic processes and a further imbalance in the mechanisms of proteostasis that may contribute to the deleterious effects of THC on cognition.

2. Materials and Methods

2.1. Animals

Adult 3-months-old male C57BL/6J mice weighting 22-25 g were used. Animals were located in cages of 4 in a controlled temperature (21 ± 1ºC) and humidity environment (55 ± 10%). They had access to water and food *ad libitum*. Lighting cycle of 12-h was maintained (from 8:00 h to 20:00 h). All the studies were carried out during the light phase. All animal procedures were conducted in accordance with standard ethical guidelines (European Communities Directive 2010/63/EU) and approved by the local ethical committee (Comitè Ètic d'Experimentació Animal-Parc de Recerca Biomèdica de Barcelona, CEEA-PRBB).

2.2. Chemicals and reagents

THC was purchased from THC Pharm GmbH (Frankfurt, Germany); ethanol, NaCl, sucrose and glycerol were purchased from Merck (Madrid, Spain); cremophor EL®, $CaCl_2$, KCl, $NaHCO_3$, $MgCl_2$, glucose, HEPES, NaPyro, NaF, NaOrth, beta-glycerolphosphate, leupeptin, aprotinin, pepstatin, phenylmethylsulfonyl fluoride, triethylammonium bicarbonate buffer, Bovine Serum Albumine (BSA), sodium dodecyl sulfate (SDS), Ethylenediaminetetraacetic acid (EDTA), anti-αtubulin and anti-synaptophysin were purchased from Sigma-Aldrich/Merck (Madrid, Spain); Tris-HCl, Tween-20, nitrocellulose membranes, DC-micro protein assay were purchased from Bio-Rad (Madrid, Spain); KH_2PO was purchased from Fluka (Madrid, Spain); acetonitrile, formic acid, tag-6 (TMT-6) reagents, nanospray source, Ultramark 1621 were purchaded from ThermoFisher Scientific (Madrid, Spain); trypsin was purchased from Promega (Madrid, Spain); Anti-GSK3β and anti-PSD95 were purchased from Cell

Signalling Technologies (Beverly, MA, USA); anti-mGluR5 was purchased from Millipore/Chemicon (Darmstadt, Germany); anti-Rpt6 was purchased from Enzo Life Science (Farmingdale, NY, USA); anti-Psmd14 was purchased from Abcam (Cambridge, MA, USA); anti-GAPDH was purchased from Santa Cruz Biotechnology (Santa Cruz, CA, USA).

2.3. Drugs and treatments

Δ^9-tetrahydrocannabinol (THC) was dissolved in vehicle solution (5% ethanol : 5% cremophor EL® : 90% saline). THC (10 mg/kg), or its vehicle, was administered intraperitoneally (i.p.) in a volume of 10 mL/kg. Hippocampal tissues were dissected 3 h after THC of vehicle injection for further analysis.

2.4. Sample preparation

Synaptosome preparation: Fresh hippocampal tissue was dounce-homogenized by 10 strokes with a loose pestle and 10 strokes with a tight pestle in 30 volumes of ice-cold synaptosome lysis buffer (in mM: 2.5 $CaCl_2$, 124 NaCl, 3.2 KCl, 1.06 KH_2PO, 26 $NaHCO_3$, 1.3 $MgCl_2$, 10 Glucose, 320 Sucrose, 20 HEPES/NaOH pH7.4) including phosphatase inhibitors (in mM: 5 NaPyro, 100 NaF, 1 NaOrth, 40 beta-glycerolphosphate) and protease inhibitors (1 μg/mL leupeptin, 10 μg/mL aprotinin, 1 μg/ml pepstatin and 1 mM phenylmethylsulfonyl fluoride). An aliquot of this crude homogenate fraction (H) was used in the synaptic enrichment characterization displayed on **Fig. 1A**. This crude homogenate was centrifuged for 1 min at 2,000 xg, 4 ºC, the supernatant was recovered (S1) and the pellet resuspended in 1 mL of synaptosome lysis buffer for further centrifugation (1 min at 2,000 xg, 4 ºC). This second supernatant

(S2) was recovered and combined with S1. Total supernatant (S1+S2) was passed through a 10 μm nitrocellulose filter and centrifuged for 1 min at 4,000 xg, 4 ºC to attain the supernatant (S3). S3 was transferred to a new tube and centrifuged for 4 min at 14,000 xg, 4 ºC. This final supernatant (S4) was discarded and the pellet was used as the synaptosomal fraction. An aliquot of this synaptosomal fraction (S) was used in the synaptic enrichment characterization displayed on **Fig. 1A**.

For proteomic analysis the synaptosomal fraction was re-suspended in 4% SDS, 0.1 M HEPES (pH=8.5). For immunoblot analysis the synaptosomal fraction was resuspended in 150 μL of synaptosome lysis buffer. All the procedure was carried out in cold. Protein concentration was measured with DC-micro protein assay (Bio Rad).

Total homogenate: Fresh hippocampal tissue was dounce-homogenized by 20 strokes with a loose pestle and 20 strokes with a tight pestle in 30 volumes of lysis buffer (150 mM NaCl, 10 % glycerol, 1 mM EDTA, 1 % TX-100, 50 mM Tris-HCl pH 7.4) with phosphatase and protease inhibitors (see above). Homogenate was mixed for 10 min at 4 ºC and then centrifuged 20 min at 16,100 xg, 4 ºC. Supernatants were recovered for further analysis. All the procedure was carried out in cold. Protein concentration was assessed by DC-micro protein assay (Bio Rad).

2.5. Tandem mass tag analysis

Synaptosomal fractions obtained from 6 THC-treated mice and 6 vehicle-treated mice were obtained in parallel and re-suspended in 4% SDS, 0.1 M HEPES (pH=8.5) before they were pooled together. Protein concentration of the THC-pooled sample and the vehicle-pooled sample were measured using DC-micro protein assay (Bio-Rad). Two

samples from each pool (100 μg each), THC (T1 and T2) and vehicle (V1 and V2), were processed in parallel as follows. First, they were subjected to trypsin (Promega) digestion following the filter-aided sample preparation (FASP) protocol as described previously [27]. Peptides generated in the digestion for all 4 samples were desalted with an Oasis Hydrophilic-Lipophilic-Balanced (HLB) cartridge (Waters, Mildford, MA, USA), evaporated to dryness, dissolved in 0.5 M triethylammonium bicarbonate buffer and labeled with tandem mass tag-6 (TMT-6) reagents (ThermoFischer Scientific) at lysines and terminal amine groups following the manufacturer's protocol. Samples from THC-treated mice were labeled with TMT-128 and TMT-129 reagents (T1 and T2, respectively), and samples from vehicle-treated mice were labeled with TMT-126 and TMT-127 reagents (V1 and V2, respectively). Each of the 4 chemical labels dissociates in the mass spectrometer to produce one of the discrete reporter ions, which intensity is measured in a MS/MS scan and provides the peaks used for peptide quantification. After labeling, all 4 samples (V1, V2, T1, T2) were pooled. The pooled sample containing labeled peptides was desalted with an Oasis HLB cartridge (Waters), evaporated to dryness and fractionated using Strong Cation Exchange and Strong Anion Exchange chromatography as described previously [27]. Fractions were passed through nanoLC in aEasyLC system (Proxeon-ThermoFisher Scientific) before running them on a Linear Trap Quadropole (LTQ) Orbitrap Velos (ThermoFisher Scientific) fitted with a nanospray source (ThermoFisher Scientific). Peptides were separated in a reverse phase column, 75 μm x 150 mm (Nikkyo Technos Co., Ltd., Tokyo, Japan) using a 5 to 35% gradient of acetonitrile with 0.1% formic acid at 0.3 μL/min for 120 min. LTQ-Orbitrap Velos was operated in positive ion mode with 2.2 kV nanospray voltage and source temperature at 325 °C. For external and internal calibration of the instrument we used Ultramark 1621 and the background polysiloxane ion signal at m/z 445.1200,

respectively. Experiments were run on the data-dependent acquisition (DDA) mode of the instrument. Full MS scans were acquired over a mass range of m/z 350-2,000 with 60,000 resolution setting for the Orbitrap mass analyzer. High energy collision dissociation (HCD) originated fragment ion spectra for the mass range of m/z 100-2,000 were acquired in the Orbitrap mass analyzer with 7,500 resolution setting. In each cycle of DDA analysis, after each survey scan, the top ten most intense ions with multiple charged ions above a threshold ion count of 10,000 were selected for fragmentation at normalized collision energy of 45%. All data were acquired with Xcalibur 2.1 software. Protein identification and quantitation was performed by Proteome Discoverer software v.1.4.0.288 (ThermoFisher Scientific). Mascot® v2.3 (Matrix Science Ltd., London, UK) was used as search engine against a mouse SwissProt database that included the most common contaminants. Settings included carbamidomethylation for cysteines, TMT for Lys and N-terminal as fixed modification, and N-terminal acetylation and methionine oxidation as variable modifications. Peptide tolerance was 7 ppm in MS and 20 mmu in MS/MS mode. The maximum number of missed cleavages was 3. Peptides with a FDR (False Discovery rate) lower than 5% were discarded and only proteins containing at least two spectra were used for subsequent quantification.

2.6. Analysis of synaptosomal proteome

The obtained hippocampal synaptosomal proteome was compared with several well-established synaptosomal, pre- and postsynaptic proteomes and a highly pure postsynaptic density (PSD) proteome obtained in the Bayés' laboratory [28–39]. Only the proteins appearing in at least one of the indicated proteomes were considered as synaptic, which were subsequently classified as (i) synaptic, when found in both pre-

and postsynaptic proteomes or in any synaptosomal proteome; (ii) postsynaptic, when absent from presynaptic proteomes; and (iii) presynaptic, when absent from postsynaptic proteomes.

2.7. Differential expression analysis

Specific protein expression was calculated using Proteome Discoverer software module for TMT quantification and the obtained ratios for the TMT reporters were normalized on protein median for each sample (V1, V2, T1, T2). The differential expression analysis comparing THC conditions and vehicle conditions was conducted using two alternative approaches. The first procedure, named "group-wise analysis", considered the intensities of both vehicle and THC groups together. We selected as differentially expressed genes in THC-treated conditions compared to vehicle-treated conditions, those with a q-value < 0.05. The second procedure, named "individual-wise analysis", was motivated by previous studies that used data from individual samples [40,41]. It consisted in pairing the determinations in each THC sample (T1 and T2) with each vehicle sample (V1 and V2), and selecting the genes located in the extremes for all the 4 potential pairings: TMT-128 (T1) vs. TMT-126 (V1); TMT-128 (T1) vs. TMT-127 (V2); TMT-129 (T2) vs. TMT-126 (V1); TMT-129 (T2) vs. TMT-127 (V2). The extremes were defined using z-score < -2 and > 2.

2.8. Network-based analysis of mouse proteome

A mouse interactome containing known physical interactions between mouse proteins was created by integrating data from IntAct [42], BioGRID [43], DIP [44] and HPRD [45] using the BIANA software [46]. In BIANA, we merged protein interactions in

different databases by using the common identifiers used by these databases (such as ENTREZ gene id) or sequence identity (exact match of the protein sequence). Then, we filtered interactions coming from pull down assays (such as Tandem Affinity Purification) and used the largest connected component of the interaction network corresponding to the mouse interactome. Then we used GUILD [47], a software to score the connectedness of the nodes in a network with respect to the seeds. Proteins of the mouse interactome were assigned an initial score of 1 or 0.01 depending on whether they were associated with the proteins modulated by THC (seeds) or not, respectively. We used NetScore algorithm that iteratively calculated the score that arrived from seeds to each node through multiple shortest paths between the node and the seeds (default parameters of 2 iterations with 3 repetitions were used). The 150 top-scoring proteins were selected for functional enrichment analysis. Gene Ontology terms significantly enriched among top-scoring proteins were identified using the FuncAssociate software [48]. The data and links of tools used in the network-based analysis are available online at http://sbi.upf.edu/data/cannabinoid_effects/.

2.9. Immunoblot

Twenty five micrograms of hippocampal homogenate protein or 10 μg of synaptosomal protein were separated in 10% SDS-polyacrylamide gel and then transferred by electrophoresis onto nitrocellulose membranes (Bio-Rad).

Membranes were blocked in 3% bovine serum albumin (BSA) dissolved in with TBS-T (100 mM NaCl, 0.1% Tween-20, 10 mM Tris, pH 7.4) for 1 hour at RT. Then, membranes were incubated during 2h with primary antibodies: anti-αtubulin (mouse monoclonal, 1:15,000), anti-GSK3β (rabbit monoclonal, 1:800), anti-PSD95 (rabbit

polyclonal, 1:500), anti-mGluR5 (rabbit polyclonal, 1:800), anti-synaptophysin (mouse monoclonal, 1:800); anti-Rpt6 (mouse monoclonal, 1:800); anti-Psmd14 (rabbit monoclonal, 1:1,000); anti-GAPDH (mouse monoclonal, 1:12,000, used as housekeeping control). Afterwards, membranes were washed three times, 4 minutes each, with T-TBS, and later incubated for 1 hour with horseradish peroxidase-conjugated anti-rabbit or anti-mouse antibodies (Pierce, diluted 1:5,000 and 1:10,000, respectively). Images of immunoreactive bands were acquire on a ChemiDoc XRS System (Bio-Rad) and quantified by The Quantity One software v4.6.3 (Bio-Rad).

2.10. 20S proteasome activity assay

Hippocampal 20S proteasome activity 3 h after THC or vehicle administration was measured using the 20S Proteasome Activity Assay Kit (APT280, Chemicon, Temecula, CA, USA) following manufacturer's instructions. The assay measures the chymotrypsin-like activity in the hippocampal homogenates, using Suc–Leu–Leu–Val–Tyr–(7-Amino-4-methylcoumarin) (LLVY-AMC) as a substrate. AMC fluorescence (380/460) released after cleavage was quantified using a fluorometer. Briefly, 40 µg of hippocampal homogenates per mouse were incubated in the presence of LLVY-AMC for 90 min at 37 ºC and then fluorescence was measured. AMC fluorescence resulting from chymotrypsin-like activity in the hippocampal samples from THC-treated mice was expressed as percentage to vehicle-treated animals.

2.11. Statistical analysis

Immunoblot and proteasome activity data were expressed as percentage of the control group ± standard deviation of the mean (SD). Data (vehicle vs. THC) were analyzed by Student's t-test. Differences were considered significant at $p<0.05$.

3. Results

3.1. Proteomic validation of synaptosomal enriched fractions

We performed a proteomic analysis of hippocampal synaptosomal fractions to obtain insights on the protein status after an acute exposure to an amnesic dose of THC (10 mg/kg, i.p.). Immunoblot experiments comparing equal amounts of protein of a crude homogenate fraction (H) and a synaptosomal fraction (S) obtained after subcellular fractionation from the same crude homogenate originated from a single hippocampus (see methods), showed that this synaptosomal fraction was enriched in presynaptic markers (synaptophysin) and postsynaptic markers (PSD95 and mGluR5) compared to cytosolic and microtubule proteins such as GSK3β or α-tubulin, respectively, that were underrepresented (**Fig 1A**).

Proteomic analysis with tandem mass tagging (TMT) [49] was performed to quantify synaptosomal proteins 3 h after THC treatment. This approach identified 2,040 proteins common to control and treated animals. The obtained synaptosomal proteome was first contrasted with eleven different well-established synaptic proteomes to confirm synaptic enrichment of the sample. Synaptic proteomes were obtained from either synaptosomes, postsynaptic densities (PSDs), synaptic vesicles (SVs) or the presynaptic active zone (AZ) [28,29,31–36,38,39]. We observed that 1,912 proteins out of the 2,040 (94%) were found in at least one of these reference proteomes. Further analysis revealed that most proteins were common to pre- and postsynaptic sites (60%), followed by PSD-specific proteins (37.3%), while only 2.7% of all proteins were presynaptic-specific (**Fig 1B**).

3.2. THC modulates the proteome content in the hippocampal synaptosomal fraction

Differential expression analysis was conducted using two alternative approaches: a group-wise and an individual-wise analysis (see methods). The differential expression study using the group-wise analysis (**Fig 2A**) revealed a significant (q-value < 0.05) alteration in the relative levels of 122 proteins, 42 increased and 80 decreased their expression (**Fig 2B**). Among these proteins, 112 proteins had been previously classified as synaptic proteins. Specifically, 71 of these proteins (58.2%) are considered general synaptic proteins, 39 (32%) are classified exclusively as PSD proteins, and 2 (1.6%) are located exclusively in the presynaptic compartment (**Fig 2C**).

We used the 122 proteins from the group-wise analysis as seeds for a network-based analysis. Then, we ran GUILD software [47] to score all the proteins in the mouse interactome based on their topological connections in the network with respect to the seeds (differentially expressed proteins). Then, we checked the functional enrichment of the top 150 highest-scoring proteins. Functional enrichment analysis showed a significant over-representation of metabolic processes involving mitochondrial physiology and cellular respiration, as well as cytoskeletal reorganization pathways (see **Table 1**).

We additionally performed a differential expression study using the individual-wise analysis. This approach revealed a pool of 28 proteins that consistently appeared at the extremes of the normal distribution of the data (z-score < 0.05 and > 0.95) (**Fig 3A**). These proteins were distributed among the different categories as follows: synaptic proteins (7 proteins, 25%; Increased: Tmsb4x, Rab8b, D430041D05Rik; Decreased: Timm8a1, Mtch1, Sel1l, Atp5j); pre-synaptic specific-proteins (1 protein, 3.6%; Decreased: Cox5a); postsynaptic specific proteins (10 proteins, 35.7%; Increased: Sfn, Krt6a, Krt42, Krt16, Dsp, Clic4; Decreased: Arsb, Mecr, Psmd14); proteins not listed in the reference proteomes (10 proteins, 35.7%; Increased: Arfip1, Atg4b, H2afz, Lsm4,

Ubxn8; Decreased: Nrgn, Riok1, Sirpb1c, Try10, Tmem44) (**Fig 3B**). We then performed a network-based analysis using those 28 proteins as seeds, and we checked the functional enrichment of top 150 highest-scoring proteins (see **Table 2**). Functional enrichment analysis revealed the proteasome complex as the top significantly enriched function (adjusted p-value < 0.05). To investigate whether the observed effect was originated either from up- or down- regulated proteins modulated by THC, we repeated the bioinformatics analysis using either the up-regulated or the down-regulated seeds separately. In this case, the proteasome system (PS) was only highlighted when down-regulated proteins were used as seeds.

3.3. THC administration decreases proteasome activity in the hippocampus

In order to address whether THC was affecting PS components in hippocampus we assessed by immunoblot the expression of two relevant components of the 19S particle [50]: Psmd14, down-regulated in our proteomics experiment, and Rpt6, a key component for proteasome activation [51]. Hippocampal samples from mice treated with THC revealed a slight but non-significant reduction in both Psmd14 (VEH: 100 ± 7.2 (n = 6), THC: 86.9 ± 7.6 (n = 6), $t(10) = 1.23$, $p = 0.25$) and Rpt6 (VEH: 100 ± 8.7 (n = 6), THC: 84.7 ± 12.6 (n = 6), $t(10) = 0.99$, $p = 0.34$) subunits referred to the housekeeping control glyceraldehyde-3-phosphate dehydrogenase (GAPDH) (**Fig 4A**).

Alternatively, we analyzed 20S proteasome activity in hippocampal samples obtained after THC or vehicle treatment using an *in vitro* assay. For this purpose, protein homogenates obtained from hippocampal tissues collected 3 h after treatment were incubated with the proteasome substrate LLVY-AMC. Under these conditions of THC treatment, there was a significant decrease in 20S proteasome activity (VEH: 100 ± 4.5

(n = 6), THC: 65.9 ± 4.8 (n = 6), $t(10) = 5.1$, $p < 0.001$) (**Fig 4B**). These data support a strong modulation of the PS activity in the hippocampus, an effect of THC administration that has not been yet identified.

4. Discussion

Our study reveals the impact of THC administration on the hippocampal synaptosomal proteome highlighting its effect on metabolic pathways, and the proteasome system, both relevant to synaptic function. The synapse, considered the functional unit of the brain, is a metabolically-demanding subcellular structure dynamically regulated to respond to local signals. These local cues can result in dramatic changes in morphology and signaling characteristics, contributing to the plastic features associated to their function in the continuously remodeling of neuronal circuits [52,53].

In this study, we revealed that a single exposure to an amnesic dose of THC changed in the hippocampus the expression of 122 proteins, 80 up-regulated and 42 down-regulated, in a time window of 3 h. Further analysis confirmed that most of the proteins obtained were previously observed in synaptic proteomes. This result, together with the immunoblot comparison between synaptosomes and homogenate samples strengthened the fact that we were working truly with synaptosomal samples. On the other hand, the finding that THC modified the expression of 122 synaptic proteins, in such a short period of time, endorsed the view of an effect on protein translation and homeostasis.

Subsequent gene-network analysis using the 122 proteins significantly modified by THC clearly pointed to a role of metabolic processes, which have been directly associated to neuroplasticity [54]. These results are in agreement with previous research showing that THC alters oxidative metabolism in brain samples [55]. Although these effects had been interpreted as a sign of neuronal damage [56,57], the recent identification of CB1 receptors in mitochondria led to the discovery of a possible new mechanism underlying THC effects. Thus, it was described how THC decreases mitochondrial activity and how this effect was linked to impairments in memory

function [26,58]. Moreover, signaling pathways acutely activated by THC at amnesic doses, such as the PI3K/Akt/GSK-3 pathway [19] have been found relevant for mitochondria functioning [59,60]. Therefore, our data are in agreement with previous observations and further support a relevant role of THC at modulating synaptic metabolism.

The individual-wise analysis of the proteomic data allowed to uncover an additional relevant pathway that could be also altered by THC. Taking into consideration those common extreme alterations observed after THC administration, we obtained a reduced number of seeds for a second protein network-based analysis. Functional enrichment analysis using the top scoring proteins revealed that the proteasome complex was perturbed by THC administration. This result was also obtained using only the down-regulated seeds, indicating a possible drop in PS functioning. Recently, the significance of proper PS activity in synaptic plasticity and memory has been put forward [61–63], and therefore it is plausible that THC may impact memory function by affecting the PS. In this regard, the PS is the major system of protein degradation machinery in eukaryotes, and there is growing evidence that proper protein degradation is as important as protein synthesis for memory formation [64,65]. The PS needs a fine regulation and adequate functioning of its regulatory subunits [66]. In this sense, Psmd14 (also known as Rpn11 or Poh1), is a crucial regulatory non-ATPase sub-unit from the 19S proteasome in charge of deubiquitinating substrates by cleavage of Lys-63-linked poly-ubitiquin chains [61]. Importantly, only deubiquitinated proteins can be processed by the 20S PS [67,68]. Indeed, deubiquitinases have been previously found to have a relevant role in synaptic function and proteostasis [62,69]. Rpt6 (a 19S AAA-ATPase) is also essential for proteasome activity as it was described to be necessary for proteasome activation and translocation to dendrites [51,70] as well as for synaptic

strength [71]. While immunoblot data only showed non-significant decreases in the expression of these PS relevant subunits after THC, we observed a significant decrease in 20S PS activity 3 h after THC administration pointing to a reduction in PS functionality mediated by THC. We cannot discard an interrelation between the main effects of THC pinpointed in this study, the modification of metabolic processes and the reduction of PS activity, given the significant ATP-dependence of the PS activity [72,73].

Notably, considering the THC-mediated decrease of PS activity in the hippocampus, which may be inter-related with the decrease in synaptic metabolism, together with previous observations that a similar dose of THC increases TORC1 signaling and protein synthesis in the hippocampus [17,18], lead to hypothesize a possible general imbalance in hippocampal synaptic proteostasis that may underlie an aberrant plasticity. This plasticity impairment prevent proper long-term plasticity leading to the amnesic effect of THC [74].

Altogether, this study supports a relevant effect of THC on synaptic metabolic processes and identifies for the first time, to the best of our knowledge, the synaptic PS as a novel mediator of the responses associated to a single administration of an amnesic dose of THC. Alterations in PS activity resulting from THC administration may contribute to the disruptive action of marijuana intoxication on learning and memory since it would either alter proteostasis networks or decrease other functional roles of the PS. Additional studies are warrant to understand the features of synaptic proteostasis alterations by THC which may underlie synaptic dysfunction and cognitive impairment.

Acknowledgements

We thank M. Pinto and F. Porrón for expert technical assistance and H. Molina for helpful comments. V.S.-M. is the recipient of a predoctoral fellowship (Ministerio de Economía y Competitividad). This study was supported by Grants from the Ministerio de Economía, Innovación y Competitividad (MINECO) (#BFU2015-68568-P (MINECO/FEDER, UE) to A.O., #BFU2015-69717-P (MINECO/FEDER, UE) to RRV and AB, #RYC-2011-08391 to AB, #SAF2017-90664-REDT to RRV and AB, #SAF2014-59648-P and #SAF2017-84060-R to R.M.; a grant from the Instituto de Salud Carlos III (#RD16/0017/0020) to R.M.; Generalitat de Catalunya (2017SGR-669 to R.M. and 2017SGR1776 to RRV and AB) and ICREA (Institució Catalana de Recerca i Estudis Avançats) Academia to A.O. and R.M. Mass spectrometric analyses were performed at the CRG/UPF Proteomics Unit which is part of the of Proteored, PRB3 and is supported by grant PT17/0019, of the PE I+D+i 2013-2016, funded by ISCIII and ERDF. Grant "Unidad de Excelencia María de Maeztu", funded by the MINECO (#MDM-2014-0370); PLAN E (Plan Español para el Estímulo de la Economía y el Empleo); FEDER funding is also acknowledged.

Conflict of interest

Authors declare no conflict of interest.

Figure legends

Figure 1. Validation of synaptosomes enriched samples. A) Characterization of synaptosomal preparation through immunoblot. Representative immunoblot and relative quantification of synaptic and cytosolic proteins (10 μg of protein per lane) in crude homogenate fraction (H) and synaptosomal fraction (S). Synaptic enrichment (left panel) for each immunodetected protein was calculated using the following formula: $(Imm_S - Imm_H) / (Imm_S + Imm_H)$, where Imm_S and Imm_H were the immunoreactive densities for each protein in each S and H sample obtained in parallel from 4 hippocampi (each preparation represented by a different symbol for every protein detected). Positive values denote enrichment of a given protein in synaptosomes while negative values denoted reduced distribution in synaptosomes. B) Characterization of the synaptosomal proteome. Out of 2,040 identified proteins, 1,911 (94%) were previously described in the reference proteomes. From this 94% synaptic proteins 60% were described as both pre- and postsynaptic proteins, 37.3% were described in PSD-specific proteomes, and 2.7% were characterized in presynaptic-specific proteomes. Blue color represents proteins already listed in reference proteomes while yellow color represents proteins not listed before in synaptic proteomes.

Figure 2. Group-wise analysis. A) Schematic drawing of the analysis performed. Fold-change and q-values were calculated using the vehicle samples as reference. The proteins with q-value below 0.05 were selected as significantly modulated proteins and used as seeds to run the network-based scoring algorithm GUILD. B) Volcano plot for the group-wise analysis after acute THC treatment. Orange dots represent protein distribution of significant alterations after THC administration (q-value < 0.05). C)

Localization of the 122 significantly modified proteins in the group-wise analysis. Among those proteins previously identified in synaptic proteomes, 71 (58.2%) had been described in pre- and postsynaptic proteomes, 39 (32%) were described specifically in PSD proteomes, 2 (1.6%) were described in pre-synaptic proteomes and 10 (8.2%) were not listed in the reference proteomes.

Figure 3. Individual-wise analysis. A) Schematic drawing of the analysis performed. THC samples were paired with vehicle samples and the proteins located in the extremes of the distributions were selected as significantly modulated. The proteins in intersection between the modulated proteins of all the distributions were used as seeds to run the network-based scoring algorithm GUILD and to obtain a ranking of the proteins in the mouse interactome that were in the neighborhood of the modulated proteins. A subnetwork of the top-150 highest-scoring proteins is represented, where a cluster of proteasome-associated proteins can be observed. B) Localization of the 28 proteins obtained in the intersection of all 4 potential comparisons (T1/V1, T1/V2, T2/V1, T2/V2). The extremes were defined using z-score < -2 and > 2. Among the 28 proteins, 7 (25%) were described as pre- and postsynaptic proteins (Up-regulated: Tmsb4x, Rab8b, D430041D05Rik; Down-regulated: Timm8a1, Mtch1, Sel1l, Atp5j); only 1 protein (3.6%) was considered specifically presynaptic (Down-regulated: Cox5a); 10 (35.7%) were considered specifically postsynaptic proteins (Up-regulated: Sfn, Krt6a, Krt42, Krt16, Dsp, Clic4; Down-regulated: Arsb, Mecr, Psmd14); finally, 10 (35.7%) proteins were not listed in the reference proteomes (Up-regulated: Arfip1, Atg4b, H2afz, Lsm4, Ubxn8; Down-regulated: Nrgn, Riok1, Sirpb1c, Try10, Tmem44).

Figure 4. THC affects the proteasome activity in the hippocampus. Mice (n = 6-8 per group) were treated with THC 10mg/kg 3 h before hippocampal tissues were dissected for analysis. (A) Immunoblot shows that THC treatment produced a non-significant decrease in the expression of Psmd14 and Rpt6 (n=6 per group). (B) Proteasome 20S chymotrypsin-like activity is decreased in animals that received THC 3 h after treatment compared to controls (n=8 per group). Dots indicate individual measures. Data are expressed as average ± S.D. *** $p < 0.001$ compared to vehicle control.

References

[1] J. Mounteney, P. Griffiths, R. Sedefov, A. Noor, J. Vicente, R. Simon, The drug situation in Europe: an overview of data available on illicit drugs and new psychoactive substances from European monitoring in 2015., Addiction. 111 (2016) 34–48. doi:10.1111/add.13056.

[2] United Nations Office on Drugs and Crime, *World Drug Report (2017).*

[3] S.P.H. Alexander, Therapeutic potential of cannabis-related drugs., Prog. Neuropsychopharmacol. Biol. Psychiatry. 64 (2016) 157–66. doi:10.1016/j.pnpbp.2015.07.001.

[4] Y. Gaoni, R. Mechoulam, Isolation, structure, and partial synthesis of an active constituent of hashish, J. Am. Chem. Soc. 86 (1964) 1646–1647. doi:10.1021/ja01062a046.

[5] R. Mechoulam, L.A. Parker, The Endocannabinoid system and the brain, Annu. Rev. Psychol. 64 (2013) 21–47. doi:10.1146/annurev-psych-113011-143739.

[6] M. Kano, T. Ohno-Shosaku, Y. Hashimotodani, M. Uchigashima, M. Watanabe, Endocannabinoid-Mediated control of synaptic transmission, Physiol. Rev. 89 (2009) 309–380. doi:10.1152/physrev.00019.2008.

[7] M. Herkenham, A.B. Lynn, M.D. Litrle, M.R. Johnsont, L.S. Melvin, B.R. De Costa, K.C. Riceo, Cannabinoid receptor localization in brain, Neurobiology. 87 (1990) 1932–1936.

[8] Y. Kawamura, M. Fukaya, T. Maejima, T. Yoshida, E. Miura, M. Watanabe, T. Ohno-Shosaku, M. Kano, The CB1 cannabinoid receptor is the major

cannabinoid receptor at excitatory presynaptic sites in the hippocampus and cerebellum., J. Neurosci. 26 (2006) 2991–3001. doi:10.1523/JNEUROSCI.4872-05.2006.

[9] J. Kim, B.E. Alger, Reduction in endocannabinoid tone is a homeostatic mechanism for specific inhibitory synapses., Nat. Neurosci. 13 (2010) 592–600. doi:10.1038/nn.2517.

[10] T. Ohno-Shosaku, M. Kano, Endocannabinoid-mediated retrograde modulation of synaptic transmission, Curr. Opin. Neurobiol. 29 (2014) 1–8. doi:10.1016/j.conb.2014.03.017.

[11] E. Hebert-Chatelain, L. Reguero, N. Puente, B. Lutz, F. Chaouloff, R. Rossignol, P.-V. Piazza, G. Benard, P. Grandes, G. Marsicano, Cannabinoid control of brain bioenergetics: Exploring the subcellular localization of the CB1 receptor., Mol. Metab. 3 (2014) 495–504. doi:10.1016/j.molmet.2014.03.007.

[12] G. Bénard, F. Massa, N. Puente, J. Lourenço, L. Bellocchio, E. Soria-Gómez, I. Matias, A. Delamarre, M. Metna-Laurent, A. Cannich, E. Hebert-Chatelain, C. Mulle, S. Ortega-Gutiérrez, M. Martín-Fontecha, M. Klugmann, S. Guggenhuber, B. Lutz, J. Gertsch, F. Chaouloff, M.L. López-Rodríguez, P. Grandes, R. Rossignol, G. Marsicano, Mitochondrial CB1 receptors regulate neuronal energy metabolism, Nat. Neurosci. 15 (2012) 558–564. doi:10.1038/nn.3053.

[13] C. Zanettini, L. V Panlilio, M. Alicki, S.R. Goldberg, J. Haller, S. Yasar, Effects of endocannabinoid system modulation on cognitive and emotional behavior., Front. Behav. Neurosci. 5 (2011) 57. doi:10.3389/fnbeh.2011.00057.

[14] M. Ranganathan, D.C. D'Souza, The acute effects of cannabinoids on memory in

humans: a review, Psychopharmacology (Berl). 188 (2006) 425–444. doi:10.1007/s00213-006-0508-y.

[15] A.H. Lichtman, K.R. Dimen, B.R. Martin, Systemic or intrahippocampal cannabinoid administration impairs spatial memory in rats, Psychopharmacology (Berl). 119 (1995) 282–290. doi:10.1007/BF02246292.

[16] L.E. Wise, A.J. Thorpe, A.H. Lichtman, Hippocampal CB(1) receptors mediate the memory impairing effects of Delta(9)-tetrahydrocannabinol., Neuropsychopharmacology. 34 (2009) 2072–80. doi:10.1038/npp.2009.31.

[17] E. Puighermanal, G. Marsicano, A. Busquets-Garcia, B. Lutz, R. Maldonado, A. Ozaita, Cannabinoid modulation of hippocampal long-term memory is mediated by mTOR signaling., Nat. Neurosci. 12 (2009) 1152–8. doi:10.1038/nn.2369.

[18] E. Puighermanal, A. Busquets-Garcia, R. Maldonado, A. Ozaita, Cellular and intracellular mechanisms involved in the cognitive impairment of cannabinoids., Philos. Trans. R. Soc. Lond. B. Biol. Sci. 367 (2012) 3254–63. doi:10.1098/rstb.2011.0384.

[19] A. Ozaita, E. Puighermanal, R. Maldonado, Regulation of PI3K/Akt/GSK-3 pathway by cannabinoids in the brain., J. Neurochem. 102 (2007) 1105–14. doi:10.1111/j.1471-4159.2007.04642.x.

[20] S.C. Borrie, H. Brems, E. Legius, C. Bagni, Cognitive dysfunctions in intellectual disabilities: the contributions of the Ras-MAPK and PI3K-AKT-mTOR pathways, Annu. Rev. Genomics Hum. Genet. 18 (2017) 115–142. doi:10.1146/annurev-genom-091416-035332.

[21] M. Costa-Mattioli, W.S. Sossin, E. Klann, N. Sonenberg, Translational control of

long-lasting synaptic plasticity and memory., Neuron. 61 (2009) 10–26. doi:10.1016/j.neuron.2008.10.055.

[22] J. Bockaert, P. Marin, mTOR in brain physiology and pathologies, Physiol. Rev. 95 (2015) 1157–1187. doi:10.1152/physrev.00038.2014.

[23] E. Santini, T.N. Huynh, E. Klann, Mechanisms of translation control underlying long-lasting synaptic plasticity and the consolidation of long-term memory, in: Prog. Mol. Biol. Transl. Sci., 2014: pp. 131–167. doi:10.1016/B978-0-12-420170-5.00005-2.

[24] J. Sanders, K. Cowansage, K. Baumga, M. Mayford, Elimination of dendritic spines with long-term memory is specific to active circuits, 32 (2012) 12570–12578. doi:10.1523/JNEUROSCI.1131-12.2012.

[25] N. Singh, J. Hroudová, Z. Fišar, Cannabinoid-induced changes in the activity of electron transport chain complexes of brain mitochondria, J. Mol. Neurosci. 56 (2015) 926–931. doi:10.1007/s12031-015-0545-2.

[26] E. Hebert-Chatelain, T. Desprez, R. Serrat, L. Bellocchio, E. Soria-Gomez, A. Busquets-Garcia, A.C. Pagano Zottola, A. Delamarre, A. Cannich, P. Vincent, M. Varilh, L.M. Robin, G. Terral, M.D. García-Fernández, M. Colavita, W. Mazier, F. Drago, N. Puente, L. Reguero, I. Elezgarai, J.-W. Dupuy, D. Cota, M.-L. Lopez-Rodriguez, G. Barreda-Gómez, F. Massa, P. Grandes, G. Bénard, G. Marsicano, A cannabinoid link between mitochondria and memory., Nature. 539 (2016) 555–559. doi:10.1038/nature20127.

[27] J.R. Wiśniewski, A. Zougman, N. Nagaraj, M. Mann, Universal sample preparation method for proteome analysis., Nat. Methods. 6 (2009) 359–62.

doi:10.1038/nmeth.1322.

[28] J. Burré, T. Beckhaus, H. Schägger, C. Corvey, S. Hofmann, M. Karas, H. Zimmermann, W. Volknandt, Analysis of the synaptic vesicle proteome using three gel-based protein separation techniques, Proteomics. 6 (2006) 6250–6262. doi:10.1002/pmic.200600357.

[29] S. Takamori, M. Holt, K. Stenius, E.A. Lemke, M. Grønborg, D. Riedel, H. Urlaub, S. Schenck, B. Brügger, P. Ringler, S.A. Müller, B. Rammner, F. Gräter, J.S. Hub, B.L. De Groot, G. Mieskes, Y. Moriyama, J. Klingauf, H. Grubmüller, J. Heuser, F. Wieland, R. Jahn, Molecular anatomy of a trafficking organelle, Cell. 127 (2006) 831–846. doi:10.1016/j.cell.2006.10.030.

[30] R. Gerlai, N. Shinsky, a Shih, P. Williams, J. Winer, M. Armanini, B. Cairns, J. Winslow, W. Gao, H.S. Phillips, Regulation of learning by EphA receptors: a protein targeting study., J. Neurosci. 19 (1999) 9538–49. http://www.ncbi.nlm.nih.gov/pubmed/10531456.

[31] G.R. Phillips, L. Florens, H. Tanaka, Z.Z. Khaing, L. Fidler, J.R. Yates, D.R. Colman, Proteomic comparison of two fractions derived from the transsynaptic scaffold., J. Neurosci. Res. 81 (2005) 762–75. doi:10.1002/jnr.20614.

[32] M. Morciano, J. Burre, C. Corvey, M. Karas, H. Zimmermann, W. Volknandt, Immunoisolation of two synaptic vesicle pools from synaptosomes: a proteomics analysis, J. Neurochem. 95 (2005) 1732–1745. doi:10.1111/j.1471-4159.2005.03506.x.

[33] À. Bayés, M.O. Collins, C.M. Galtrey, C. Simonnet, M. Roy, M.D. Croning, G. Gou, L.N. van de Lagemaat, D. Milward, I.R. Whittle, C. Smith, J.S. Choudhary,

S.G. Grant, Human post-mortem synapse proteome integrity screening for proteomic studies of postsynaptic complexes, Mol. Brain. 7 (2014) 88. doi:10.1186/s13041-014-0088-4.

[34] U. Distler, M.J. Schmeisser, A. Pelosi, D. Reim, J. Kuharev, R. Weiczner, J. Baumgart, T.M. Boeckers, R. Nitsch, J. Vogt, S. Tenzer, In-depth protein profiling of the postsynaptic density from mouse hippocampus using data-independent acquisition proteomics, Proteomics. 14 (2014) 2607–2613. doi:10.1002/pmic.201300520.

[35] O. Engmann, J. Campbell, M. Ward, K.P. Giese, A.J. Thompson, Comparison of a protein-level and peptide-level labeling strategy for quantitative proteomics of synaptosomes using isobaric tags., J. Proteome Res. 9 (2010) 2725–33. doi:10.1021/pr900627e.

[36] À. Bayés, M.O. Collins, R. Reig-Viader, G. Gou, D. Goulding, A. Izquierdo, J.S. Choudhary, R.D. Emes, S.G.N. Grant, Evolution of complexity in the zebrafish synapse proteome, Nat. Commun. 8 (2017) 14613. doi:10.1038/ncomms14613.

[37] R. Reig-Viader, À. Bayés, Quantitative in-depth profiling of the postsynaptic density proteome to understand the molecular mechanisms governing synaptic physiology and pathology, in: Humana Press, New York, NY, 2017: pp. 255–280. doi:10.1007/978-1-4939-7119-0_16.

[38] B.A. Györffy, P. Gulyássy, B. Gellén, K. Völgyi, D. Madarasi, V. Kis, O. Ozohanics, I. Papp, P. Kovács, G. Lubec, Á. Dobolyi, J. Kardos, L. Drahos, G. Juhász, K.A. Kékesi, Widespread alterations in the synaptic proteome of the adolescent cerebral cortex following prenatal immune activation in rats, Brain. Behav. Immun. 56 (2016) 289–309. doi:10.1016/J.BBI.2016.04.002.

[39] J. Zhou, Z. Liu, J. Yu, X. Han, S. Fan, W. Shao, J. Chen, R. Qiao, P. Xie, Quantitative proteomic analysis reveals molecular adaptations in the hippocampal synaptic active zone of chronic mild stress-unsusceptible rats., Int. J. Neuropsychopharmacol. 19 (2015) pyv100. doi:10.1093/ijnp/pyv100.

[40] H. Wang, Q. Sun, W. Zhao, L. Qi, Y. Gu, P. Li, M. Zhang, Y. Li, S.-L. Liu, Z. Guo, Individual-level analysis of differential expression of genes and pathways for personalized medicine., Bioinformatics. 31 (2015) 62–8. doi:10.1093/bioinformatics/btu522.

[41] J. Menche, E. Guney, A. Sharma, P.J. Branigan, M.J. Loza, F. Baribaud, R. Dobrin, A.-L. Barabási, Integrating personalized gene expression profiles into predictive disease-associated gene pools., NPJ Syst. Biol. Appl. 3 (2017) 10. doi:10.1038/s41540-017-0009-0.

[42] S. Orchard, M. Ammari, B. Aranda, L. Breuza, L. Briganti, F. Broackes-Carter, N.H. Campbell, G. Chavali, C. Chen, N. del-Toro, M. Duesbury, M. Dumousseau, E. Galeota, U. Hinz, M. Iannuccelli, S. Jagannathan, R. Jimenez, J. Khadake, A. Lagreid, L. Licata, R.C. Lovering, B. Meldal, A.N. Melidoni, M. Milagros, D. Peluso, L. Perfetto, P. Porras, A. Raghunath, S. Ricard-Blum, B. Roechert, A. Stutz, M. Tognolli, K. van Roey, G. Cesareni, H. Hermjakob, The MIntAct project—IntAct as a common curation platform for 11 molecular interaction databases, Nucleic Acids Res. 42 (2014) D358–D363. doi:10.1093/nar/gkt1115.

[43] A. Chatr-Aryamontri, R. Oughtred, L. Boucher, J. Rust, C. Chang, N.K. Kolas, L. O'Donnell, S. Oster, C. Theesfeld, A. Sellam, C. Stark, B.-J. Breitkreutz, K. Dolinski, M. Tyers, The BioGRID interaction database: 2017 update., Nucleic

Acids Res. 45 (2017) D369–D379. doi:10.1093/nar/gkw1102.

[44] L. Salwinski, C.S. Miller, A.J. Smith, F.K. Pettit, J.U. Bowie, D. Eisenberg, The Database of interacting proteins: 2004 update, Nucleic Acids Res. 32 (2004) 449D–451. doi:10.1093/nar/gkh086.

[45] T.S. Keshava Prasad, R. Goel, K. Kandasamy, S. Keerthikumar, S. Kumar, S. Mathivanan, D. Telikicherla, R. Raju, B. Shafreen, A. Venugopal, L. Balakrishnan, A. Marimuthu, S. Banerjee, D.S. Somanathan, A. Sebastian, S. Rani, S. Ray, C.J. Harrys Kishore, S. Kanth, M. Ahmed, M.K. Kashyap, R. Mohmood, Y.L. Ramachandra, V. Krishna, B.A. Rahiman, S. Mohan, P. Ranganathan, S. Ramabadran, R. Chaerkady, A. Pandey, Human protein reference database: 2009 update, Nucleic Acids Res. 37 (2009) D767–D772. doi:10.1093/nar/gkn892.

[46] J. Garcia-Garcia, E. Guney, R. Aragues, J. Planas-Iglesias, B. Oliva, Biana: a software framework for compiling biological interactions and analyzing networks, BMC Bioinformatics. 11 (2010) 56. doi:10.1186/1471-2105-11-56.

[47] E. Guney, B. Oliva, Exploiting protein-protein interaction networks for genome-wide disease-gene prioritization, PLoS One. 7 (2012). doi:10.1371/journal.pone.0043557.

[48] G.F. Berriz, J.E. Beaver, C. Cenik, M. Tasan, F.P. Roth, Next generation software for functional trend analysis, Bioinformatics. 25 (2009) 3043–3044. doi:10.1093/bioinformatics/btp498.

[49] A. Thompson, J. Schäfer, K. Kuhn, S. Kienle, J. Schwarz, G. Schmidt, T. Neumann, R. Johnstone, A.K.A. Mohammed, C. Hamon, Tandem mass tags: a

novel quantification strategy for comparative analysis of complex protein mixtures by MS/MS., Anal. Chem. 75 (2003) 1895–904. http://www.ncbi.nlm.nih.gov/pubmed/12713048 (accessed June 21, 2018).

[50] Z.C. Gu, C. Enenkel, Proteasome assembly, Cell. Mol. Life Sci. 71 (2014) 4729–4745. doi:10.1007/s00018-014-1699-8.

[51] B. Bingol, C.F. Wang, D. Arnott, D. Cheng, J. Peng, M. Sheng, Autophosphorylated CaMKIIα acts as a scaffold to recruit proteasomes to dendritic spines, Cell. 140 (2010) 567–578. doi:10.1016/j.cell.2010.01.024.

[52] M. Mayford, S.A. Siegelbaum, E.R. Kandel, Synapses and memory storage., Cold Spring Harb. Perspect. Biol. 4 (2012) a005751–a005751. doi:10.1101/cshperspect.a005751.

[53] K.M. Harris, R.J. Weinberg, Ultrastructure of synapses in the mammalian brain., Cold Spring Harb. Perspect. Biol. 4 (2012) a005587–a005587. doi:10.1101/cshperspect.a005587.

[54] M.P. Mattson, M. Gleichmann, A. Cheng, Mitochondria in neuroplasticity and neurological disorders, Neuron. 60 (2008) 748–766. doi:10.1016/j.neuron.2008.10.010.

[55] P. Chiu, R. Karler, C. Craven, D.M. Olsen, S.A. Turkanis, The influence of delta9-tetrahydrocannabinol, cannabinol and cannabidiol on tissue oxygen consumption., Res. Commun. Chem. Pathol. Pharmacol. 12 (1975) 267–86. http://www.ncbi.nlm.nih.gov/pubmed/1197914 (accessed June 1, 2018).

[56] B. Costa, M. Colleoni, Changes in rat brain energetic metabolism after exposure to anandamide or Δ9-tetrahydrocannabinol, Eur. J. Pharmacol. 395 (2000) 1–7.

doi:10.1016/S0014-2999(00)00170-9.

[57] V. Wolff, A.-I. Schlagowski, O. Rouyer, A.-L. Charles, F. Singh, C. Auger, V. Schini-Kerth, C. Marescaux, J.-S. Raul, J. Zoll, B. Geny, Tetrahydrocannabinol induces brain mitochondrial respiratory chain dysfunction and increases oxidative stress: a potential mechanism involved in cannabis-related stroke, Biomed Res. Int. 2015 (2015) 1–7. doi:10.1155/2015/323706.

[58] V. Rangaraju, N. Calloway, T.A. Ryan, Activity-Driven Local ATP Synthesis Is Required for Synaptic Function, Cell. 156 (2014) 825–835. doi:10.1016/j.cell.2013.12.042.

[59] T. Zheng, X. Yang, D. Wu, S. Xing, F. Bian, W. Li, J. Chi, X. Bai, G. Wu, X. Chen, Y. Zhang, S. Jin, Salidroside ameliorates insulin resistance through activation of a mitochondria-associated AMPK/PI3K/Akt/GSK3β pathway, Br. J. Pharmacol. 172 (2015) 3284–3301. doi:10.1111/bph.13120.

[60] R. Xu, Q. Hu, Q. Ma, C. Liu, G. Wang, The protease Omi regulates mitochondrial biogenesis through the GSK3β/PGC-1α pathway, Cell Death Dis. 5 (2014) e1373–e1373. doi:10.1038/cddis.2014.328.

[61] T.J. Jarome, R.K. Devulapalli, The Ubiquitin-proteasome system and memory: moving beyond protein degradation, Neurosci. (2018) 107385841876231. doi:10.1177/1073858418762317.

[62] J.R. Kowalski, P. Juo, The Role of deubiquitinating enzymes in synaptic function and nervous system diseases, Neural Plast. 2012 (2012) 1–13. doi:10.1155/2012/892749.

[63] A.N. Hegde, Proteolysis, synaptic plasticity and memory, Neurobiol. Learn.

Mem. 138 (2017) 98–110. doi:10.1016/j.nlm.2016.09.003.

[64] J. Artinian, A.-M.T. Mcgauran, X. De Jaeger, L. Mouledous, B. Frances, P. Roullet, X. De Jaeger, L. Mouledous, B. Frances, P. Roullet, Protein degradation , as with protein synthesis , is required during not only long-term spatial memory consolidation but also reconsolidation, Eur. J. Neurosci. 27 (2008) 3009–3019. doi:10.1111/j.1460-9568.2008.06262.x.

[65] D.S. Reis, T.J. Jarome, F.J. Helmstetter, Memory formation for trace fear conditioning requires ubiquitin-proteasome mediated protein degradation in the prefrontal cortex, Front. Behav. Neurosci. 7 (2013) 1–7. doi:10.3389/fnbeh.2013.00150.

[66] K. Tanaka, The proteasome: From basic mechanisms to emerging roles, Keio J. Med. 62 (2013) 1–12. doi:10.2302/kjm.2012-0006-RE.

[67] B.-H. Lee, D. Finley, R.W. King, A high-throughput screening method for identification of inhibitors of the deubiquitinating enzyme USP14, in: Curr. Protoc. Chem. Biol., John Wiley & Sons, Inc., Hoboken, NJ, USA, 2012: pp. 311–30. doi:10.1002/9780470559277.ch120078.

[68] S.A.H. de Poot, G. Tian, D. Finley, Meddling with fate: the proteasomal deubiquitinating enzymes, J. Mol. Biol. 429 (2017) 3525–3545. doi:10.1016/j.jmb.2017.09.015.

[69] A.N. Hegde, The ubiquitin-proteasome pathway and synaptic plasticity, Learn. Mem. 17 (2010) 314–327. doi:10.1101/lm.1504010.

[70] T.J. Jarome, N.C. Ferrara, J.L. Kwapis, F.J. Helmstetter, CaMKII regulates proteasome phosphorylation and activity and promotes memory destabilization

following retrieval, Neurobiol. Learn. Mem. 128 (2016) 103–109. doi:10.1016/j.nlm.2016.01.001.

[71] S.N. Djakovic, E.M. Marquez-lona, S.K. Jakawich, R. Wright, C. Chu, M.A. Sutton, G.N. Patrick, Phosphorylation of Rpt6 regulates synaptic strength in hippocampal neurons, J. Neurosci. 32 (2012) 5126–5131. doi:10.1523/JNEUROSCI.4427-11.2012.

[72] G. Lehmann, R.G. Udasin, A. Ciechanover, On the linkage between the ubiquitin-proteasome system and the mitochondria., Biochem. Biophys. Res. Commun. 473 (2016) 80–86. doi:10.1016/j.bbrc.2016.03.055.

[73] G.A. Collins, A.L. Goldberg, The logic of the 26S proteasome., Cell. 169 (2017) 792–806. doi:10.1016/j.cell.2017.04.023.

[74] T.V.P. Bliss, G.L. Collingridge, R.G.M. Morris, Synaptic plasticity in health and disease: introduction and overview, Philos. Trans. R. Soc. B Biol. Sci. 369 (2013) 20130129–20130129. doi:10.1098/rstb.2013.0129.

A

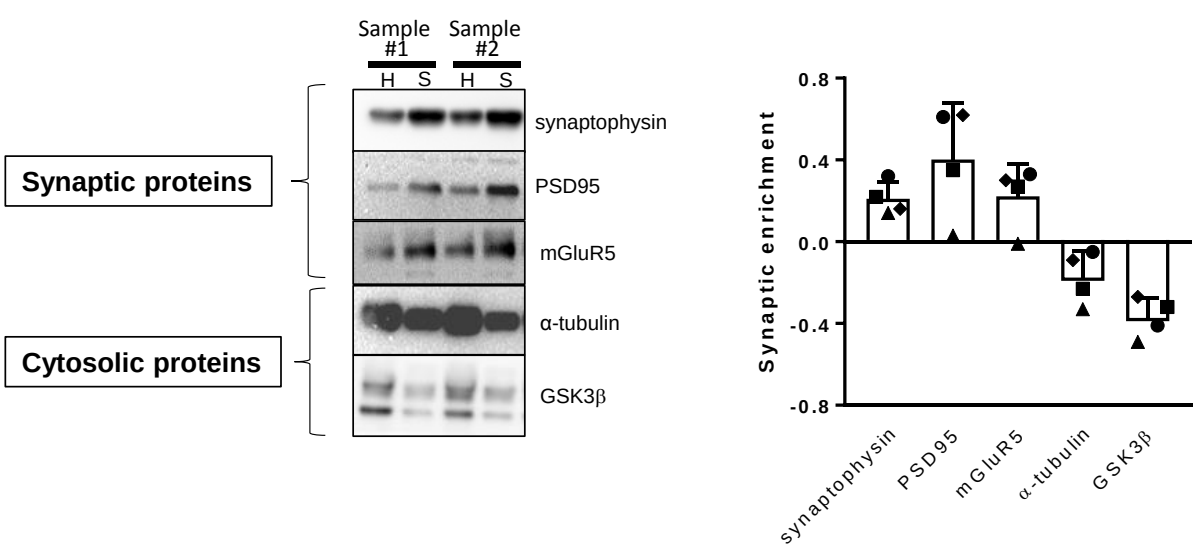

B

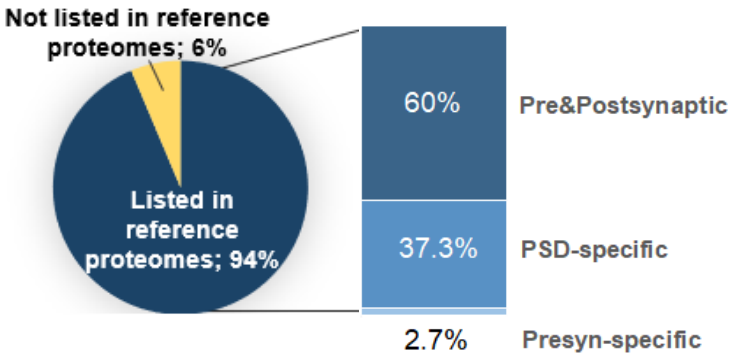

Salgado-Mendialdua_BCP-S-18-00873R_Figure 1

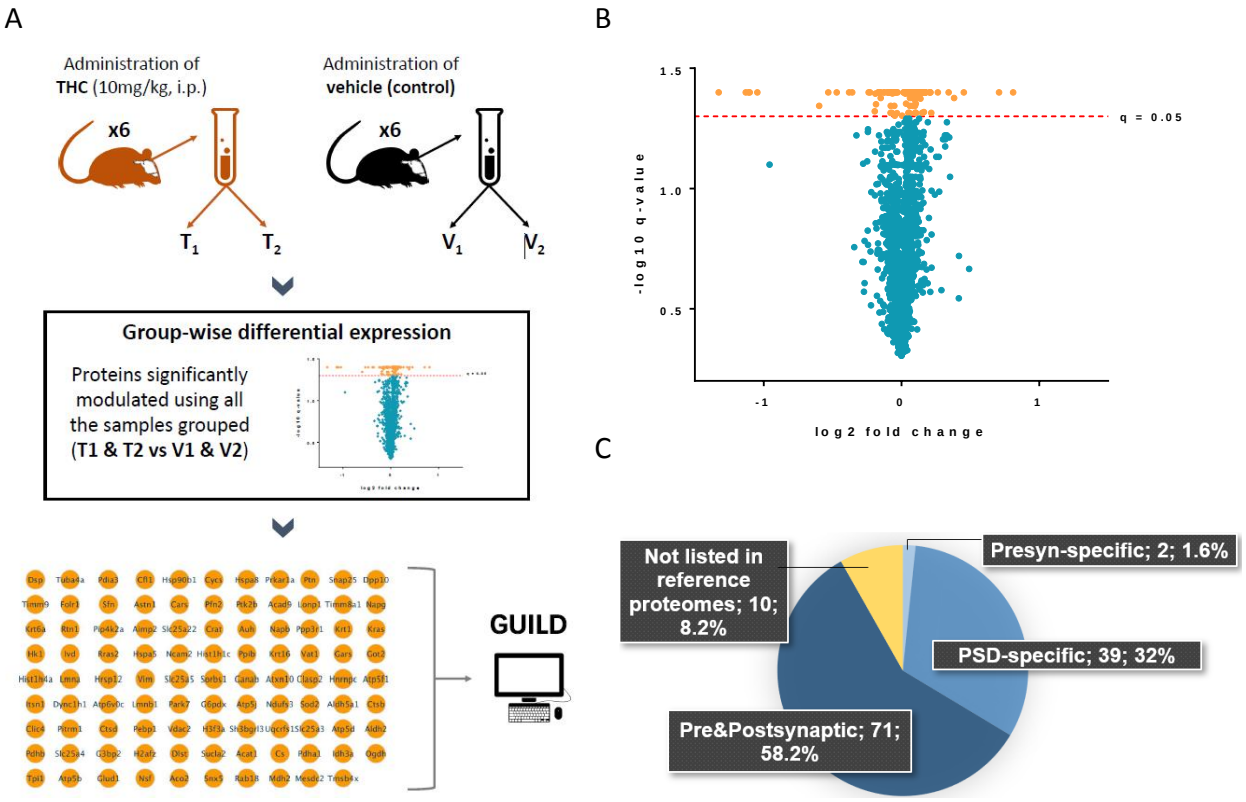

Salgado-Mendialdua_BCP-S-18-00873R_Figure 2

A

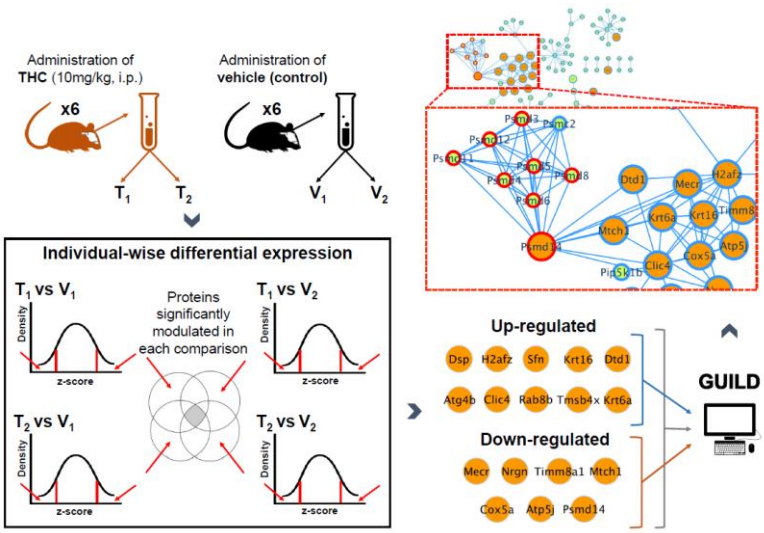

B

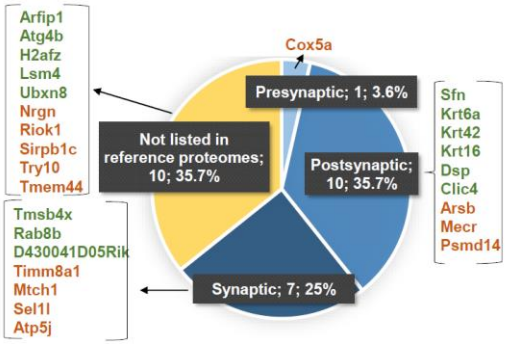

Salgado-Mendialdua_BCP-S-18-00873R_Figure 3

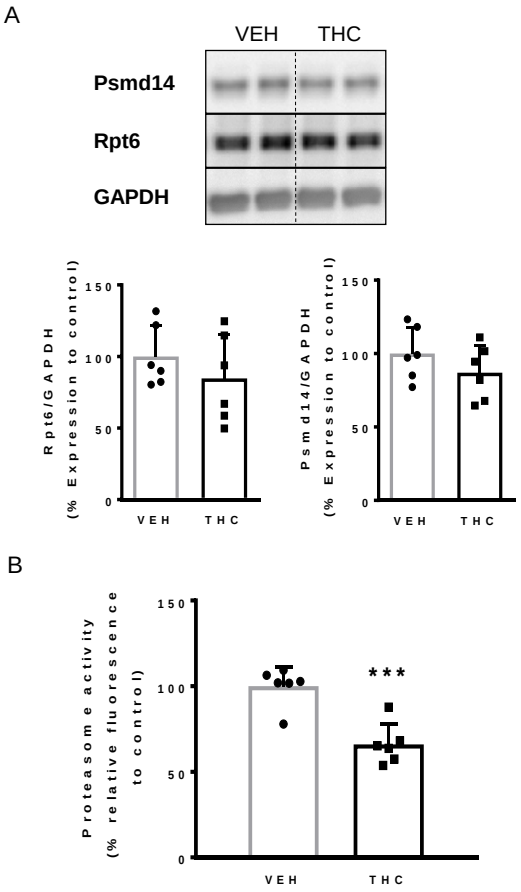

Salgado-Mendialdua_BCP-S-18-00873R_Figure 4